Trends in Applied Sciences Research

ISSN 1819-3579

Academic
Journals Inc.

www.academicjournals.com

Trends in Applied Sciences Research 4 (4): 216-228, 2009
ISSN 1819-3579

Effect of Milling Parameters on Frictions when Milling Hastelloy C-22HS: A FEM and Statistical Method

[1]K. Kadirgama, [1]M.M. Noor, [1]M.M. Rahman,
[2]K.A. Abou-El-Hossein, [3]B. Mohammad and [3]H. Habeeb
[1]Automotive Excellence Center, Universiti Malaysia Pahang,
26300 UMP, Kuantan, Pahang, Malaysia
[2]Department of Mechatronics, Nelson Mandela Metropolitan University,
Port Elizabeth 6301, South Africa
[3]Department of Mechanical Engineering,
Universiti Tenaga Nasional, Kajang, Selangor, Malaysia

Abstract: This study was developed the Finite Element Model (FEM) and Response Surface Method (RSM) to investigate the effect of milling parameters on frictions when milling Hastelloy C-22HS. This study gain better understanding of the friction distribution in metal cutting process. The RSM was used to minimize the number of simulation. The contour plot from RSM shows the relationship between input variables including the cutting speed, feed rate and axial depth and responses including the friction coefficient, friction angle, friction stress and friction force. Feed rate, axial depth and cutting speed play major role to generate high friction coefficient, friction angle, friction stress and friction force. When all the variables at highest value the friction stress become larger, on the other hand reduce the feed rate and increase other variable, it cause high friction coefficient, angle and force. The combination of numerical analysis and statistical method are very useful to analysis the distribution of friction in milling. It is suitable to use middle value of cutting speed, feed rate and axial depth when milling same type of materials.

Key words: Finite element analysis, response surface method, milling, friction, Hastelloy C-22HS

INTRODUCTION

Milling is typically used to produce parts that are not axially symmetric and have many features such as holes, slots, pockets and even three dimensional surface contours. Parts that are fabricated completely through milling often include components that are used in limited quantities, perhaps for prototypes, such as custom designed fasteners or brackets. The milling process requires a milling machine, workpiece, fixture and cutter. The workpiece is a piece of pre-shaped material that is secured to the fixture, which itself is attached to a platform inside the milling machine. The cutter is a cutting tool with sharp edge that is also secured in the milling machine and rotates at high speed. By feeding the workpiece into the rotating cutter, material is cut away from this workpiece in the form of small chips to create the desired shape. The direct experimental approach to study machining process is expensive and time consuming, especially when a wide range of parameters is included: tool geometry,

Corresponding Author: K. Kadirgama, Automotive Excellence Center, Universiti Malaysia Pahang, 26300 UMP, Kuantan, Pahang, Malaysia

materials, cutting conditions, etc. The alternative approaches are mathematical simulations where numerical methods are applied. The finite element methods are most frequently used (Mackerle, 2003). The goal of finite element studies are to derive a computational model predicting the deformations, stresses and strains in the workpiece, as well as the loads on tool working under specific cutting parameters (Mackerle, 2003). Ueda and Manabe (1993) used a numerical approach and simulated the chip formation in the cutting process. Lovell *et al*. (1998) introduced an explicit dynamic FEM method to simulate orthogonal cutting with sharp edge but a restricted contact cutting tool. Friction conditions at the chip-tool interface in early FEM models of metal cutting have been largely ignored (Klamecki, 1973; Tay *et al*., 1974). Carroll and Strenkowski (1988) assumed to be constant with a coefficient of friction based on Coulomb's law at the entire chip-tool interface. Shih *et al*. (1990) introduced a model that consists of the sticking region for which the friction force is constant and the sliding region for which friction force varies linearly according to Coulomb's law. Usui and Shirakashi (1982) performed rigid-plastic FE simulations of steady state orthogonal cutting process. The mechanistic approach has been widely used for the force predictions and also been extended to predict associated machine component deflections and form errors (Kline *et al*., 1982, 1983; Sutherland and DeVor, 1986; Budak and Altintas, 1994, 1995). Another alternative is to use mechanics of cutting approach to determine the milling force coefficients as used by Armarego and Whitifeld (1985). In this approach, an oblique cutting force model together with an orthogonal cutting database is used to predict milling force coefficients (Budak *et al*., 1996). This approach was applied to the cases of complex milling cutter geometries and multi-axis milling operations (Altintas and Lee, 1996; Altintas and Engin, 2001; Ozturk and Budak, 2005). Interfacial friction on tool rake face is not continuous and is a function of the normal and frictional stress distributions. The normal stress is greatest at tool tip and gradually decreases to zero at point where the chip separates from the rake face (Zorev, 1963). As shown in Fig. 1, shape of the secondary plastic zone in the sticking region can be assumed triangular according to Tay *et al*. (1974). On the rake face point N is located at interface between the sticking and sliding regions. Line MN is an II slip-line that is assumed to be straight. Oxley (1989) was proposed similar approach proposed to analyze the hydrostatic stresses along MN. The researchers developed an

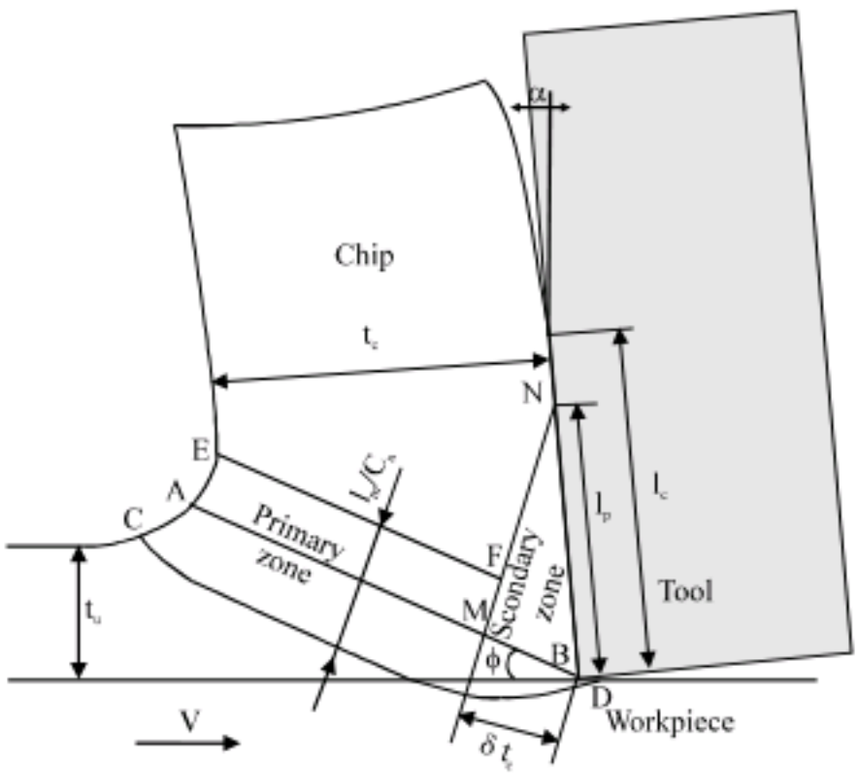

Fig. 1: Simplified deformation zones in orthogonal cutting

analytical model to predict the cutting forces, average temperatures and stresses in the primary and secondary deformation zones by using:

- Flow stress of the work material as a function of strain and velocity-modified temperature which couples strain rate to temperature
- Thermal properties of the work material
- Tool geometry
- Cutting conditions

On the contrary, friction model becomes strategically important when other variables are considered, such as shear angle, normal pressure and thermal effects even if either normal pressure or temperature were found with accuracy using shear model too. In fact, the success and reliability of numerical models are heavily dependent upon work material flow stress, friction parameters between the tool and work material interfaces, the fracture criterion and the thermal parameters (Childs, 2006). Tay *et al*. (1974) were proposed an experimentally determined the slip-line field of secondary deformation zone, which is used to determine the shearing stress k_{int} in the sticking region and coefficient of friction μ in the sliding region. The objective of this study is to develop the frictions parameters using statistical and FEM method. The models will be indicated the relationship between milling variables (cutting speed, federate and axial depth) with frictions parameters (friction coefficient, friction angle, friction stress and friction force).

MATERIALS AND METHODS

This study was conducted at Advanced Machining laboratory, Department of Mechanical Engineering, Universiti Tenaga Nasional. The duration of the project is July 2007 to June 2009.

Finite Element Model

The finite element model is composed of a deformable workpiece and a rigid tool. The tool penetrates through the workpiece at a constant speed and feed rate. The model assumes plane-strain condition since generally depth of cut is much greater than feed rate. Thirdwave AdvantEdge was used with six-noded quadratic triangular elements to developed the finite element model. AdvantEdge is an automated program and it is suitable to input process parameters to develop a two-dimensional simulation of orthogonal cutting operation. The workpiece material of HASTELLOY C-22HS and cutting inserts of coated carbide grade with a TiAlN (PVD-KC520M) were used in this study. The geometry parameters of the tool were controlled accordingly to International Organization for Standardization (ISO) SPHX1205ZCFRGN1W as shown in Fig. 2. The nose radius of the inserts is 90°, clearance angle 11° and positive rake angle. Every one pass (80 mm), the simulation stopped. The spindle speed can be determined from Eq. 1:

$$\text{Spindle speed (rpm)} = \frac{\text{Cutting speed (m min}^{-1})\times 1000}{\text{Diameter of cutter (mm)}\times \pi} \quad (1)$$

AdvantEdge was used an analytical formulation for material modeling. In a typical machining event, the primary and secondary shear zones very high strain rates are achieved,

Fig. 2: KC520M insert

while the remainder of the workpiece deforms at moderate or low strain rates. In order to account for this, Thirdwave AdvantEdge incorporates a stepwise variation of the rate sensitivity exponent which is expressed as either Eq. 2:

$$\bar{\sigma} = \sigma_f\left(\varepsilon^p\right)\cdot\left(1+\frac{\dot{\varepsilon}^p}{\dot{\varepsilon}_o^p}\right)^{1/m_2}, \text{ if } \dot{\varepsilon} \le \dot{\varepsilon}_t^p \tag{2}$$

where, $\bar{\sigma}$ is the effective von Mises stress, σ_f is the flow stress, ε^p is the accumulated plastic strain, $\dot{\varepsilon}_o^p$ is a reference plastic strain rate, m_1 and m_2 are low and high strain-rate sensitivity exponents, respectively and $\dot{\varepsilon}_t$ is the threshold strain rate which separates the two regimes. In calculations, a local Newton-Raphson iteration is used to compute $\dot{\varepsilon}_o^p$ according to the low-rate equation and switches to the high rate equation if the result lies above $\dot{\varepsilon}_t$.

The von Mises stress (σ_f) can be rewrite as Eq. 3:

$$\sigma_f = \sigma_0\cdot\psi(T)\cdot\left(1+\frac{\varepsilon^p}{\varepsilon_0^p}\right)^{1/n} \tag{3}$$

where, T is the current temperature, σ_0 is the initial yield stress at reference temperature T_0, ε_0^p is the reference plastic strain, n is the hardening exponent and $\psi(T)$ is the thermal softening factor.

In the present study, it is assumed that the tool is not plastifying. Hence, it is considered as rigid. Heat can be transferred to the tool only from the workpiece. The separation of nodes, thus forming the chip from the workpiece during a cutting simulation is achieved by continuous remeshing. Therefore, during metal cutting the workpiece material is allowed to flow around the cutting tool edge and when the elements in this vicinity become distorted and lose accuracy, Thirdwave AdvantEdge alleviates element distortion by updating the finite element mesh periodically by refining large elements, remeshing distorted elements and coarsening small elements. The initial position of the workpiece and cutting tool with selected mesh is shown in Fig. 3. The initial coolant temperature is selected as the room temperature. Since, flood coolant is selected heat flux due to coolant is applied to all exposed and noncontacting surfaces on tool and workpiece, except the bottom face of the workpiece and the faces on the tool where constant temperature is applied.

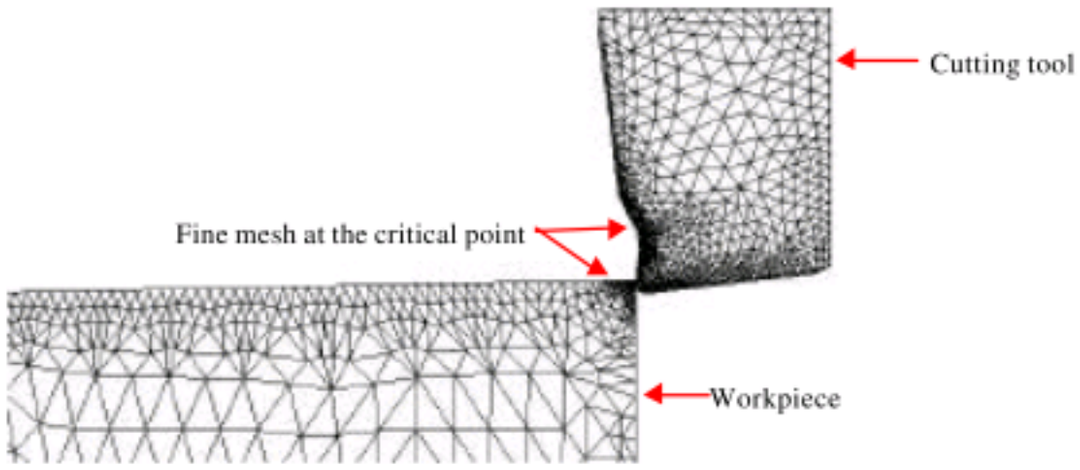

Fig. 3: Initial position of the workpiece and cutting tool with selected

Response Surface Method

The RSM is a combination of experimental and regression analysis and statistical inferences. The concept of a response surface involves a dependent variable (y) called the response variable and several independent variables $x_1, x_2, \ldots, x_k$ (Schey, 2000; Montgomery, 2001). If all of these variables are assumed to be measurable, the response variable can be expressed as Eq. 4.

$$y = f(x_1; x_2; \ldots; x_k) \tag{4}$$

where, ($x_1 = \ln V$), feed ($x_2 = \ln f$), axial depth ($x_3 = \ln a_x$) that optimize response. The observed response (y) as a function of the speed, feed rate and axial depth can be written as Eq. 5 (Schey, 2000; Montgomery, 2001):

$$y = m \times \text{Cutting speed} + n \times \text{Feed rate} + p \times \text{Axial depth} + C \tag{5}$$

where, y is the response, C, m, n and p are constants.

Equation 5 can also be written in Eq. 6:

$$y = \beta_0 x_0 + \beta_1 x_1 + \beta_2 x_2 + \beta_3 x_3 \tag{6}$$

where, $x_0 = 1$(dummy variables), x_1= cutting speed, x_2= Feed rate and x_3= Axial depth $\beta_0 = C$ and β_1, β_2 and β_3, are the model parameters.

Whilst the properties of the materials were not coincident except for tensile strength, some materials machined by a tool with a chamfer have been found to result in microstructure change because of temperature effect (Wu and Matsumoto, 1990; Matsumoto *et al*., 1986). Boothroyd (1975) and El Baradie (1993) were investigated the effect of speed, feed and depth of cut on steel and grey cast iron and then emphasized the use of RSM in developing a surface roughness prediction model.

Wu (1964) were proposed a prediction model by using Takushi method and RSM. By using the factors including the cutting speed, feed and depth of cut, Alauddin *et al*. (1998) were developed the surface roughness models and to determine the cutting conditions for 190 BHN steel and Inconel 718. The authors found that the variations of tool angles have important effects on surface roughness. In order to model and analyze the effect of each variable and minimize the cutting tests, surface roughness models utilizing response surface methodology and the experimental design were carried out in this investigation. Some key

Table 1: Level of independence variables

Levels	Low	Medium	High
Coding	-1.0	0.00	1.0
Speed, v (m min^{-1})	100.0	140.00	180.0
Feed, f (mm rev^{-1})	0.1	0.15	0.2
Axial depth, d_a (mm)	1.0	1.50	2.0

Table 2: Simulation condition

Simulation No.	Cutting speed	Feedrate	Axial depth
1	140	0.10	2.0
2	140	0.20	1.0
3	100	0.15	1.0
4	100	0.15	2.0
5	140	0.15	1.5
6	100	0.10	1.5
7	180	0.10	1.5
8	180	0.15	2.0
9	180	0.20	1.5
10	140	0.20	2.0
11	180	0.15	1.0
12	140	0.15	1.5
13	140	0.10	1.0
14	100	0.20	1.5
15	140	0.15	1.5

features of BBD include allow efficient estimation of first- and second-order terms, desirable design properties of orthogonal blocks, less expensive to run compared to CCD having the same number of factors, all the design points fall within the safe operation zones and all factors are never set to their extreme (low or high) levels, simultaneously. The suitable levels of the factors were used to deduce the design parameters as shown in Table 1 and 2 after run some preliminary run. In this study, 3 variables have been selected such as the cutting speed, feed rate and axial depth. For the radial depth, 3.5 mm was selected for every experiment.

RESULTS

The component of the resultant cutting force (R) resolved on the primary shear plane generates the shear force per unit area (k) adequate to cause the primary flow. The direction of friction angle (λ) of resultant cutting force to the normal of rake face is measurement of the average friction interaction (friction angle) between the chip and tool. The values of cutting force (F_c) and thrust force (F_t) are taken from the simulation results are shown in Table 3. Simulation results for experiment number 5 and 9 are shown in Fig. 4 and 5, respectively. A minimal description of chip formation is shown in Fig. 6. The friction angle (λ) and average friction coefficient ($\mu_{av} = \tan \lambda$), shear stress (k) and average friction stress (τ) between the chip and tool, relative to k, can be estimated with F_c and F_t the force per unit cutting edge engagement length (Childs, 2006). The average friction coefficient, shear stress and ratio of average friction stress to shear stress are expressed in Eq. 7-9, respectively:

$$\mu_{av} \equiv \tan \lambda = \frac{F_c \sin \alpha + F_t \cos \alpha}{F_c \cos \alpha - F_t \sin \alpha} \tag{7}$$

$$k = \frac{(F_c \cos \phi - F_t \sin \phi) \sin \phi}{a_c} \tag{8}$$

Table 3: Simulations results

Cutting speed (m min^{-1})	Feed rate (mm rev^{-1})	Axial depth (mm)	Cutting force F_c (N)	Thrust force F_t (N)
140	0.20	1.0	452	414
180	0.15	1.0	311	275
100	0.20	1.5	656	557
180	0.20	1.5	639	503
140	0.10	1.0	241	229
140	0.10	2.0	467	452
180	0.10	1.5	371	352
140	0.20	2.0	800	771
180	0.15	2.0	609	533
140	0.15	1.5	472	398
100	0.15	2.0	592	492
100	0.10	1.5	357	344
100	0.15	1.0	295	247
140	0.15	1.5	472	398
140	0.15	1.5	472	398

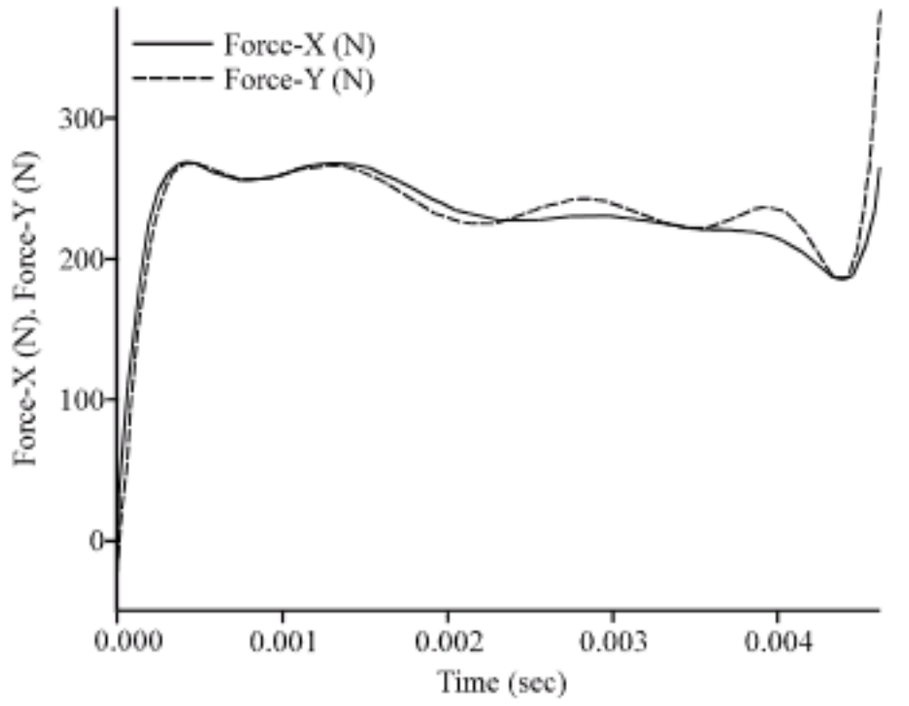

Fig. 4: Force simulation result for experiment No. 5

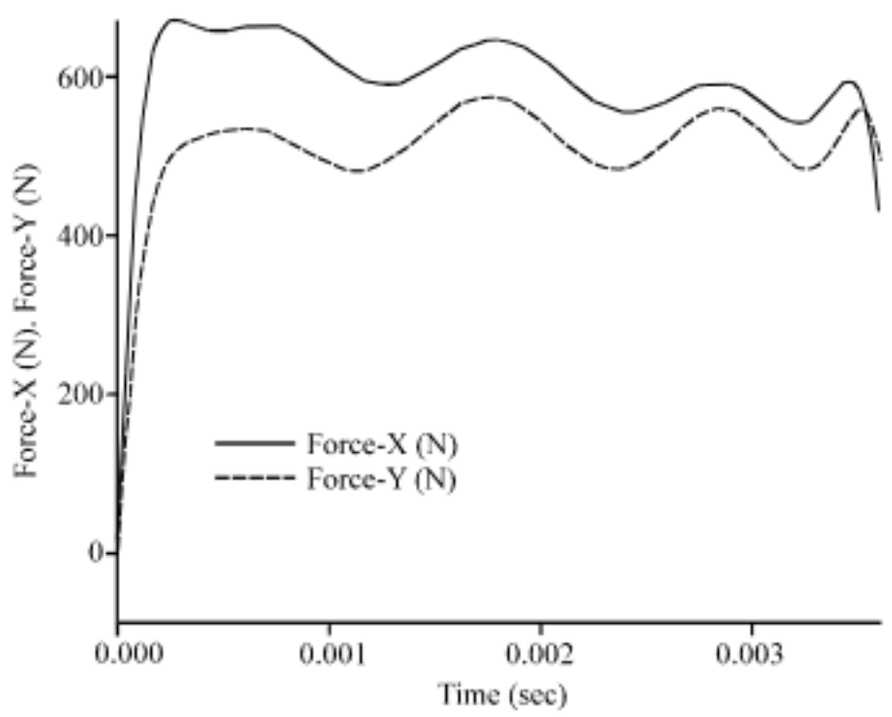

Fig. 5: Force simulation result for experiment No. 9

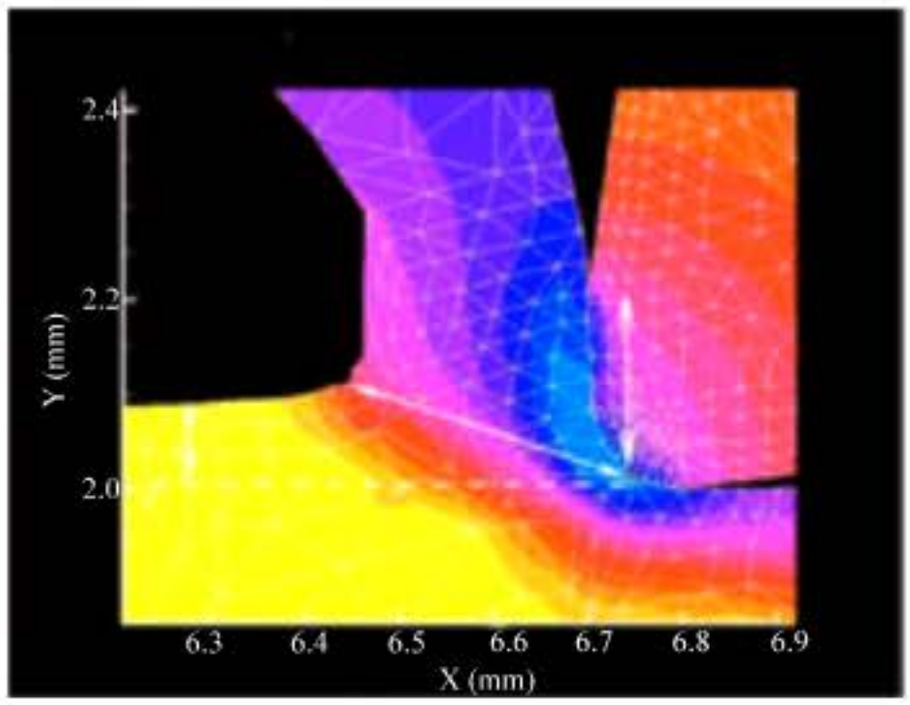

Fig. 6: A minimal description of chip formation

$$\frac{\tau}{k} = \frac{F_c \sin\alpha + F_t \cos\alpha}{(F_c \cos\phi - F_t \sin\phi)\sin\phi} \cdot \frac{a_c}{l_{OB}} \tag{9}$$

where, ϕ is the shear angle, α is the rake angle, a_c is the uncut chip thickness and l_{OB} is the contact length between the cutting tool and chip. In the simplest case, deformation takes place by intense shearing in a plane, the shear plane, inclined by shear angle (ϕ). The chip thus formed has a thickness (h_a). The shear angle determines the cutting ratio, r_c (Childs, 2006), which can be expressed as Eq. 10.

$$r_c = \frac{a_c}{h_a} \tag{10}$$

where, h_a is the chip thickness.

In milling, Eq. 11 can be used to estimated h and assume h_a will equal to feed rate (Budak, 2005).

$$h = c \cdot \sin\theta \tag{11}$$

where, c is the feed rate and θ is the angular position. The angular position can be defined as Eq. 12 (Abou-El-Hossein *et al*., 2007).

$$\theta = \Omega t \tag{12}$$

where, Ω is the angular speed (rad sec^{-1}) or $\Omega = 2\pi m/60$, n is the spindle speed in rpm and t is the time. The value of r_c gives valuable clues regarding the efficiency of the process.

From the geometry of the process, the shear angle is defined as Eq. 13 (Budak, 2005):

$$\tan\phi = \frac{r_c \cos\alpha}{1 - r_c \sin\alpha} \tag{13}$$

In deformation processes one of the contacting materials (the workpiece) deforms and doing so slides against the harder surface (cutting tool). A frictional stress, τ is again

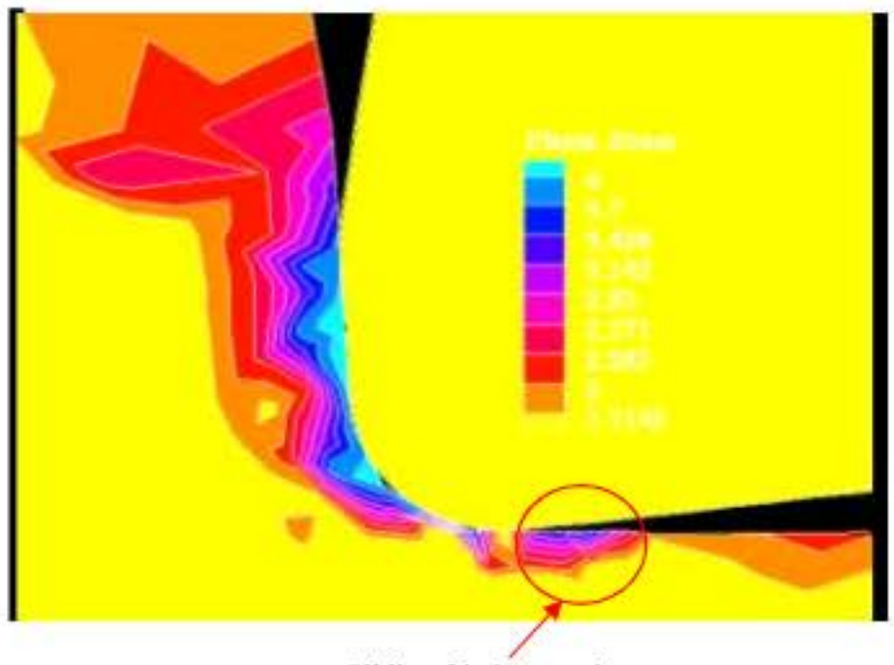

Fig. 7: Sticking friction

generated, but this time there is a limit to μ, because the material will choose a deformation pattern that minimizes the energy of deformation (Boothroyd, 1975). If friction is high, interface shear stress τ will reach, in the limit, the shear flow stress τ_s of the workpiece material. At this point, the workpiece refuses to slide on the tool surface; instead, it deforms by shearing inside the body. In general, it is more accurate to say that the coefficient of friction becomes meaningless when $\tau_i = \tau_f$, since there is no relative sliding at the interface. This is described as sticking friction as shown in Fig. 7, even though the workpiece does not actually stick to the workpiece. From the point of view of forces acting on the tool, the resultant force F_r may be regarded as being composed of the normal force F_n acting perpendicular to the tool face and the friction force F acting along the face. Their magnitude may be calculated from simulation forces and the rake angle (Boothroyd, 1975):

$$F = f_c \sin\alpha + F_t \cos\alpha \tag{14}$$

DISCUSSION

The calculated friction coefficient, friction angle, friction stress and friction force using Eq. 4-6 and 11 are shown in Table 4. After run the 15 simulation, the average friction coefficient, friction angle, friction stress and friction force values used to find the parameters appearing in the postulated first order model Eq. 14. To do the calculation of these parameters, the method of least squares is used with the aid of Minitab. The first order linear equation of friction parameters are expressed as Eq. 15-18:

$$\text{Friction coefficient: } y_1 = 1.33 + 0.0005x_1 - 0.6x_2 + 0.0425x_3 \tag{15}$$

$$\text{Friction angle: } y_2 = 52.5650 + 0.0170x_1 - 17.1x_2 + 0.7825x_3 \tag{16}$$

$$\text{Friction stress: } y_3 = 521.5053 + 4.3x_1 + 2552.45x_2 + 802.1x_3 \tag{17}$$

$$\text{Friction force: } y_4 = 79.0859 + 0.8172x_1 - 265.02x_2 + 227.40x_3 \tag{18}$$

Table 4: The calculated friction coefficient, friction angle, friction stress and friction force

Cutting speed (m min^{-1})	Feed rate (mm rev^{-1})	Axial depth (mm)	Friction coefficient	Friction angle (°C)	Friction stress (MPa)	Friction force (N)
140	0.20	1.0	1.40	54.46	2626.06	498.95
180	0.15	1.0	1.35	53.47	1756.14	33.67
100	0.20	1.5	1.30	52.43	3585.53	681.25
180	0.20	1.5	1.20	50.19	3288.92	624.90
140	0.10	1.0	1.46	55.59	1442.70	274.11
140	0.10	2.0	1.49	56.13	2838.10	539.24
180	0.10	1.5	1.45	55.40	2218.21	421.46
140	0.20	2.0	1.48	55.95	4844.84	920.52
180	0.15	2.0	1.34	53.26	3410.53	648.00
140	0.15	1.5	1.29	52.21	2565.58	487.46
100	0.15	2.0	1.27	51.78	3180.85	604.36
100	0.10	1.5	1.48	55.95	2161.71	410.72
100	0.15	1.0	1.28	52.00	1594.48	302.95
140	0.15	1.5	1.29	52.21	2565.58	487.46
140	0.15	1.5	1.29	52.21	2565.58	487.46

Table 5: Analysis of Variance (ANOVA) for friction coefficient

Source	df	Seq SS	Adj SS	Adj MS	F-value	p-value
Regression	3	0.013625	0.013625	0.004542	0.49	0.694
Linear	3	0.013625	0.013625	0.004542	0.49	0.694
Residual error	11	0.101268	0.101268	0.009206		
Lack of fit	9	0.091468	0.091468	0.010163	2.07	0.367
Pure error	2	0.009800	0.009800	0.004900		
Total	14	0.114893				

Table 6: Analysis of Variance for friction angle

Source	df	Seq SS	Adj SS	Adj MS	F-value	p-value
Regression	3	10.758	10.758	3.586	1.00	0.428
Linear	3	10.758	10.758	3.586	1.00	0.428
Residual error	11	39.387	39.387	3.581		
Lack of fit	9	30.873	30.873	3.430	0.81	0.666
Pure error	2	8.514	8.514	4.257		
Total	14	50.145				

Table 7: Analysis of Variance for friction stress

Source	df	Seq SS	Adj SS	Adj MS	F-value	p-value
Regression	3	1653804	1653804	551268	0.67	0.590
Linear	3	1653804	1653804	551268	0.67	0.590
Residual error	11	9106668	9106668	827879		
Lack of fit	9	8459687	8459687	939965	2.91	0.282
Pure error	2	646982	646982	323491		
Total	14	10760473				

From these linear equations, one can easily notice that the response y_1, y_2, y_3 and y_4 (Friction coefficient, Friction angle, Friction stress, Friction force) is affected significantly by the feed rate followed by axial depth of cut and then by cutting speed. Generally, the increase in feed rate, axial depth and cutting speed causes the friction stress to become larger. On the other hand, the decrease in feed rate and increase in cutting speed and axial depth causes friction coefficient, friction angle and friction force increase gradually. The adequacy of the first-order model is verified using the Analysis of Variance (ANOVA). At a level of confidence of 95%, the model is checked for its adequacy. Analysis of variance for friction coefficient, friction angle, frictional stress and friction force are given in Table 5-8, respectively. It can be observed from Tables 5 to 8 that p-values of 0.367, 0.666, 0.282 and 0.206 (>0.05) are not significant with the lack-of fit and F-statistic are 2.07, 0.81, 2.91 and 4.23. This implies that the model could fit and it is adequate (Abou-El-Hossein *et al*., 2007; Kadirgama *et al*., 2008). The prediction error for cutting (tangential) force is drastically lower

Table 8: Analysis of Variance for friction force

Source	DF	Seq SS	Adj SS	Adj MS	F-value	p-value
Regression	3	113373	113373	37791	0.89	0.477
Linear	3	113373	113373	37791	0.89	0.477
Residual error	11	467781	467781	42526		
Lack of fit	9	444424	444424	49380	4.23	0.206
Pure error	2	23357	23357	11678		
Total	14	581154				

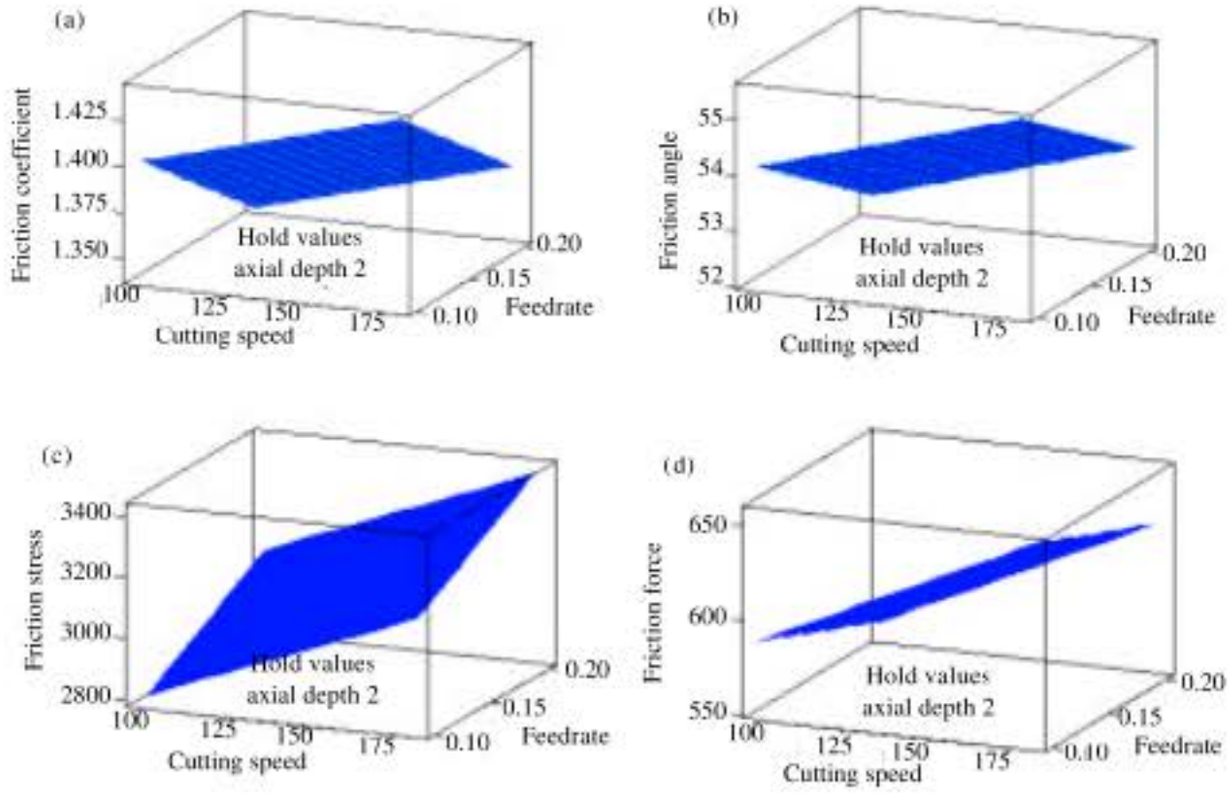

Fig. 8: (a) Friction coefficient, (b) friction angle, (c) friction stress and (d) frictional force contours in the cutting speed-feed rate plane for axial depth 2 mm

than feed force when fully sliding or fully sticking conditions are assumed in friction modeling (Filice *et al*., 2007). It is a well known phenomenon that the apparent friction coefficient increases with increases of rake angle. Simulations using the proposed model are conducted for AISI 1050 steel with coated carbide tool for different rake angles at cutting speed and feed rate of 300 m min^{-1} and 0.1 mm rev^{-1}, respectively (Ozlu *et al*., 2007; Budak and Ozlu, 2008).

The developed linear model Eq. 15-18 were used to plot contours of the friction coefficient, friction angle, friction stress, friction force at different axial depth of cut, respectively. Figure 8a-d show the friction coefficient, friction angle, friction stress, friction force contours at cutting speed-feed rate plane for axial depth 2 mm. It is clearly seen that the increase of cutting speed, feed rate and axial depth causes the friction stress increase dramatically. Meanwhile, the friction coefficient, angle and force increases with decreases of feed rate and increases of cutting speed and axial depth. Kadirgama *et al*. (2009) indicated that the feed rate was the most dominant cutting condition on the cutting force, followed by the axial depth, radial depth of cut and then by the cutting speed. The cutting force increases with increasing the feed rate, depths of cut but decreases with increasing cutting speed.

CONCLUSION

The milling parameters cutting speed, feed rate and axial depth play the major role to produce the high fiction force, coefficient, angle and stress. High friction generates heat. From the first order model, the responses (friction coefficient, friction angle, friction stress and friction force) are affected significantly by feed rate followed by axial depth of cut and

then cutting speed. The increases of friction stress increasing of feed rate, axial depth and cutting speed. On the other hand, friction coefficient, friction angle and friction force increases gradually with decreases in feed rate and increases of cutting speed and axial depth. The combination of numerical analysis and statistical method are very useful to analysis the distribution of friction in milling. It is suitable to use moderate value of cutting speed, feed rate and axial depth when milling same type of materials. When use very low feed rate, it cause higher friction coefficient, friction angle and force.

ACKNOWLEDGMENT

The authors would like to express their deep gratitude to Universiti Tenaga Nasional (UNITEN for provided the laboratory facilities and financial support by Malaysian Government through MOSTI under Project No. 03-99-03-0011-EA 0041.

REFERENCES

Abou-El-Hossein, K.A., K. Kadirgama, M. Hamdi and K.Y. Benyounis, 2007. Prediction of cutting force in end-milling operation of modified AISI P20 tool steel. J. Mater. Process. Technol., 182: 241-247.

Alauddin, M., M.A. Mazid, M.A. El-Baradi and M.S.J.Hashmi, 1998. Cutting forces in the end milling of Inconel 718. J. Mater. Process. Technol., 77: 153-159.

Altintas, Y. and P. Lee, 1996. A general mechanics and dynamics model for helical end mills. CIRP. Ann. Manuf. Technol., 45: 59-64.

Altintas, Y. and S. Engin, 2001. Generalized modeling of mechanics and dynamics of milling cutters. CIRP. Ann. Manuf. Technol., 50: 25-30.

Armarego, E.J.A. and R.C. Whitfeld, 1985. Computer based modeling of popular machining operations for force and power predictions. Ann. CIRP., 34: 65-69.

Boothroyd, G., 1975. Fundamentals of Metal Machining and Machine Tools. 1st Edn., Scripta Book Company, Washington, DC., ISBN: 0-07-006498-9, pp: 112.

Budak, E. and E. Ozlu, 2008. Development of a thermomechanical cutting process model for machining process simulations. CIRP Ann. Manuf. Technol., 57: 97-100.

Budak, E. and Y. Altintas, 1994. Identification of peripheral milling conditions for improved dimensional accuracy. Int. J. Mach. Tool Manuf., 30: 907-918.

Budak, E. and Y. Altintas, 1995. Modeling and avoidance of static deformations in peripheral milling of plates. Int. J. Mach. Tool Manuf., 35: 459-476.

Budak, E., 2005. Analytical models for high performance milling. Part I: Cutting forces, structural deformations and tolerance integrity. Int. J. Mach. Tools Manuf., 46: 1478-1488.

Budak, E., Y. Altintas and E.J.A. Armarego, 1996. Prediction of milling force coef?cients from orthogonal cutting data. J. Engin. Ind., 118: 216-224.

Carroll, J.T. and J. Strenkowski, 1988. Finite element models of orthogonal cutting with application to single point diamond turning. Int. J. Mech. Sci., 30: 899-920.

Childs, T.H.C., 2006. Friction modelling in metal cutting. Wear, 260: 310-318.

El-Baradie, M.A., 1993. Surface roughness model for turning grey cast iron (154BHN). J. Eng. Manuf., 207: 43-54.

Filice, L., F. Micari, S. Rizzuti and D. Umbrello, 2007. A critical analysis on the friction modeling in orthogonal machining. Int. J. Mach. Tools Manuf., 47: 709-714.

Kadirgama, K., K.A. Abou-El-Hossein, B.Mohammad, Habeeb Al-Ani and M.M. Noor, 2008. Cutting force prediction model by FEA and RSM when machining hastelloy C-22HS with 900 holder. Int. J. Scientific Ind. Res., 6: 421-427.

Kadirgama, K., M.M. Noor, M.M. Rahman, R.A. Bakar and B. Mohammad, 2009. Experimental and numerical study of cutting force in end-milling operation using statistical method. Proceedings of the 12th CIRP International Conference Modelling Machining Operations, May 7-8, Donostia-San Sebastian, Spain, pp: 843-850.

Klamecki, B.E., 1973. Incipient chip formation in metal cutting-a three dimension finite element analysis. Ph.D. Thesis, University of Illinois at Urbana-Champaign.

Kline, W.A. , R.E. DeVor and I.A. Shareef, 1982. The prediction of surface accuracy in end milling. J. Engng. Industry, 104: 272-278.

Kline, W.A., R.E. DeVor and I.A. Shareef, 1983. The effect of runout on cutting geometry and forces in end milling: Influence du faux rond sur la géométrie et sur les forces de coupe dans le fraisage en bout. Int. J. Mach. Tool Design Res., 23: 123-140.

Lovell, M.R., S. Bhattacharya and R. Zeng, 1998. Modeling orthogonal machining process for variable tool-chip interfacial friction using explicit dynamic finite element methods. Proceedings of the CIRP. International Workshop on Modeling of Machining Operations, (MMO'98), Atlanta, USA., pp: 265-276.

Mackerle, J., 2003. Finite element analysis and simulation of machining: An addendum a bibliography (1996–2002). Int. J. Machine Tools Manuf., 43: 103-114.

Matsumoto, Y., M.M. Barash and C.R. Liu, 1986. Effect of hardness on the surface integrity of AISI 4340 steel. ASME J. Eng. Ind., 108: 169-175.

Montgomery, D.C., 2001. Design and Analysis of Experiments. 5th Edn., John Wiley and Sons, New York, ISBN: 047148735X.

Oxley, P.L.B., 1989. Mechanics of Machining, an Analytical Approach to Assessing Machinability. Ellis Horwood Ltd., UK., ISBN: 0135686687.

Ozlu, E., E. Budak and A. Molinari, 2007. Thermomechanical modeling of orthogonal cutting including the effect of stick-slide regions on the rake face. Proceedings of the 10th CIRP International Workshop Modeling Machining Operations, Aug. 27-28, Calabria, Italy, pp: 1-8.

Ozturk, E. and E. Budak, 2005. Modeling of 5-axis milling forces. Proceedings of the 8th CIRP International Workshop Model Machining Operations, May 10-11, Chemnitz, Germany, pp: 319-332.

Schey, J.A., 2000. Introduction to Manufacturing Processes. 3rd Edn., McGraw Hill, NewYork, ISBN: 9780070311367.

Shih, A.J., S. Chandrasekar and H.T. Yang, 1990. Finite element simulation of metal cutting process with strain-rate and temperatures effects. Fund. Issues Mach. ASME., 43: 11-24.

Sutherland, J.W. and R.E. DeVor, 1986. An improved method for cutting force and surface error prediction in ?exible end milling systems. J. Engng. Ind., 108: 269-279.

Tay, A.O., M.G. Stevenson, and G. Devahldavis, 1974. Using the finite element method to determine temperature distributions in orthogonal machining. Proc. Inst. Mech. Eng., 188: 627-638.

Ueda, K. and K. Manabe, 1993. Rigid-plastic FEM analysis of three-dimensional deformations field in the chip formation process. General Assembly CIRP, 42: 35-38.

Usui, E. and T. Shirakashi, 1982. Mechanics of machining -from descriptive to predictive theory. In on the art of cutting metals-75 years later. ASME, 7: 13-35.

Wu, S.M., 1964. Tool life testing by response surface methodology. Trans. ASME B, 86: 105-116.

Wu, W. and Y. Matsumoto, 1990. The effect of hardness on residual stresses in orthogonal machining of AISI 4340 steel. J. Eng. Ind., 112: 252-259.

Zorev, N.N., 1963. Inter-relationship between shear processes occurring along tool face and shear plane in metal cutting. Int. Res. Produc. Eng., ASME., pp: 42-49.